Eye and Brain Dovepress

Open Access Full Text Article ORIGINAL RESEARCH

Peripapillary Retinal Nerve Fiber Layer (pRNFL) Thickness – A Novel Biomarker of Neurodegeneration in Late-Infantile CLN2 Disease

Nikolaos Gkalapis[1,2,*], Simon Dulz[1,*], Carsten Grohmann[1], Miriam Nickel[3], Christoph Schwering[3], Eva Wibbeler[3], Martin Stephan Spitzer[1], Angela Schulz[3], Yevgeniya Atiskova[1]

[1]Department of Ophthalmology, University Medical Center Hamburg-Eppendorf, Hamburg, Germany; [2]Department of Ophthalmology, University Hospital of Martin Luther University Halle/Wittenberg, Halle (Saale), Germany; [3]Department of Pediatrics, University Medical Center Hamburg-Eppendorf, Hamburg, Germany

*These authors contributed equally to this work

Correspondence: Yevgeniya Atiskova, Department of Ophthalmology, University Medical Center Hamburg-Eppendorf, Martinistraße 52, Hamburg, 20246, Germany, Tel +49 (0) 40 7410 – 52301, Fax +49 (0) 40 7410 – 42301, Email y.atiskova@uke.de

Purpose: To investigate the presence of peripapillary retinal nerve fiber layer (pRNFL) degeneration in patients with late-infantile neuronal ceroid lipofuscinosis type 2 (CLN2) disease and to evaluate the role of optical coherence tomography (OCT) assessed pRNFL thickness as a biomarker for CLN2 disease progression.

Patients and Methods: Forty eyes of 20 patients with genetically and enzymatically confirmed diagnosis of late-infantile CLN2 disease were included in this retrospective cohort study. All patients received 300 mg of intracerebroventricular enzyme replacement treatment (cerliponase alfa) once every two weeks. OCT imaging was performed under general anesthesia using spectral domain OCT (Heidelberg Engineering, Heidelberg, Germany). PRNFL thickness and central retinal thickness (CRT) values were manually confirmed with the Heidelberg Eye Explorer software. Corresponding pediatric data were extracted from the DEM-CHILD database. Spearman correlation coefficient values (rs) were calculated between pRNFL and CRT values, age at examination, the Weill Cornell Late Infantile Neuronal Ceroid Lipofuscinosis (Weill Cornell LINCL) Scale and the Hamburg Motor and Language (HML) Scale.

Results: Fourteen of 20 patients underwent serial examinations resulting in a total of 84 OCT Scans and 42 Weill Cornell LINCL and HML Scale scores. Mean age was 6.90 years and mean follow-up time was 1.38 years. Mean global pRNFL (G-pRNFL) thickness was 77.02 µm presenting a significant decrease compared to normative values from healthy children (106.45 µm; $p < 0.0001$). G-pRNFL displayed significant correlations towards age at examination ($r_s = -0.557$, $p < 0.01$), the Weill Cornell LINCL Scale ($r_s = 0.849$, $p < 0.01$), and the HML Scale ($r_s = 0.833$, $p < 0.01$). Repeated measurements indicated decreases in pRNFL thickness over time in most patients.

Conclusion: Patients with late-infantile CLN2 disease exhibit early onset progressive pRNFL loss regardless of outer retinal degeneration, highlighting the potential of pRNFL as an independent ocular biomarker for retinal pathology in late-infantile CLN2 disease.

Keywords: neuronal ceroid lipofuscinosis, optic nerve, optical coherence tomography, retina, neurodegeneration, eye

Introduction

The term neuronal ceroid lipofuscinoses (NCLs) encompasses a heterogenous collection of 13 distinct neurodegenerative lysosomal storage diseases (CLN 1–14) that collectively represent the most common inherited neurodegenerative disorders in childhood.[1] These disorders are attributed to mutations in genes that code for enzymes that precipitate in the accumulation of lysosomal storage material, primarily in cells of the central nervous system (CNS), causing neuron

Received: 11 April 2024
Accepted: 23 September 2024
Published: 13 November 2024

and interneuron loss.[2] CLN2 disease mainly presents as a late-infantile onset NCL (LINCL) and is associated with mutations to the tripeptidyl peptidase 1 (*TPP1*) gene, that encodes the lysosomal soluble enzyme hydrolase TPP1. Mutations to the *TPP1* gene trigger decreased activity of TPP1, resulting in the systematic accumulation of curvilinear profiles in lysosomal residual bodies. Cells of the CNS and the retina are especially vulnerable to these metabolic changes, which ultimately lead to their degeneration.[3] Symptoms usually begin in early childhood, around 2–4 years of age and include decline of verbal language, loss of motor skills, dementia, and seizures.[4] The 2–3 years following onset of symptoms are characterized by rapid deterioration of motor function, language, and swallowing, with many patients experiencing premature death in early adolescence. Ocular symptoms are a cardinal feature of late-infantile CLN2 disease, as vision loss typically manifests after 3 years of age, usually subsequently to seizures and psychomotor decline.[5] The vision loss progresses to blindness over time. However, optical coherence tomography (OCT) imaging has enabled the detection of preliminary signs of retinal degeneration in patients as young as 2 years of age, before the display of clinical ocular symptoms. The retinopathy in late-infantile CLN2 patients has been described as a bilateral, symmetric, outer retinal degeneration that expands from the central macula to the peripheral retina. This degeneration, which is especially accelerated between 4 and 6 years of age, primarily affects the retinal pigment epithelium (RPE) and photoreceptor cells in a bull's eye pattern (bull's eye maculopathy).[6–8] Currently, intracerebroventricular (ICV) enzyme replacement therapy (ERT) with recombinant human TPP1 (rhTPP1) (cerliponase alfa, Brineura, BioMarin Pharmaceuticals, California, USA) is the only United States Food and Drug Administration (US FDA) and European Medicines Agency (EMA) approved treatment for CLN2 that has proven to decelerate the progression of motor and language function decline.[9] However, the progression of retinal degeneration has only been mitigated through preclinical treatment strategies that target the retina directly. In particular, intravitreal (IVT) therapies in canine CLN2 models,[10–12] and as of recently, continuous IVT delivery of rhTPP1 in human CLN2 patients,[13] have displayed promising results in slowing down this process. Various OCT biomarkers, among them central retinal thickness (CRT), ellipsoid zone (EZ) integrity and outer nuclear layer (ONL) thickness, have been described as indicators of late-infantile CLN2 disease progression,[3,14] and therefore may support the development and monitoring of new disease-modifying treatments.

Retinal nerve fiber layer (RNFL) thickness is an extensively studied OCT biomarker in neurodegenerative disorders. Particularly, peripapillary RNFL (pRNFL) thinning has been associated with poor disease progression in a multitude of neurodegenerative diseases including Alzheimer's disease, multiple sclerosis and Parkinson's disease.[15–22] As late-infantile CLN2 disease is associated with abundant outer retinal degeneration,[6,7,15] little attention has been given to the inner retinal morphology in this neurodegenerative disease. The aim of the present retrospective, observational study was to examine the presence of pRNFL degeneration in cerliponase alfa treated patients with late-infantile CLN2 disease.

As our findings were indicative of progressive pRNFL degeneration, we furthermore evaluated pRNFL changes in correlation to neurological deterioration, as assessed via the Weill Cornell Late Infantile Neuronal Ceroid Lipofuscinoses (Weill Cornell LINCL) Scale,[5] and the Hamburg Motor and Language (HML) Scale.[23]

Materials and Methods

This is a retrospective observational study based on analysis of medical history data, as well as pediatric, neurologic, and ophthalmologic examinations performed during standard of care routine consultation visits at the University Medical Center Hamburg-Eppendorf and the NCL specialty clinic at the Department of Pediatrics and at the department of Ophthalmology. The protocol of this study was approved by the local ethical committee of the Ärztekammer Hamburg, Hamburg (PV7215) and informed consent was obtained for all patients prior to enrollment. The principles of the Declaration of Helsinki were followed. The study protocol was registered at ClinicalTrials.org (registration number: NCT04613089).

Design and Participants

Our study comprised a total of 20 patients with genetically and enzymatically confirmed diagnosis of CLN2 disease. Patient's detailed demographic and genotype data are illustrated in Table 1. All patients were treated with 300 mg of cerliponase alfa during the course of the study, administered through ICV infusions once every two weeks. The ages at which cerliponase alfa treatments were started are provided in Table 1.

Table 1 Patients' Detailed Demographic, Genotypic and Clinical Information

ID	Gender	Genotype	Age at First Brineura Treatment (years)	Age at Examination (years)	Duration of Treatment (Years)	Weill Cornell LINCL Scale Score	HML Scale Score
P1	Male	c.622C>T	3.25	6.83	3.58	6	3
				7.33	4.08	6	3
				8.25	5.00	4	2
P2	Male	c.622C>T	3.92	4.42	0.50	9	5
P3	Female	c.622C>T/ c.1678_1679del	5	7.75	2.75	2	0
P4	Female	c.617G>A	5.08	8.33	3.25	9	4
				9.33	4.25	9	4
P5	Female	c.225A>G	6.75	8.17	1.42	3	2
P6	Female	c.509-1G>C/ c.622C>T	5.08	9.25	4.17	5	2
				10.17	5.08	5	2
				11.00	5.92	5	2
P7	Male	c.622C>T	3.75	5.17	1.42	5	2
				7.00	3.25	2	0
P8	Male	c.622C>T/ c.509–1G>C	4.92	6.75	1.83	0	0
				7.67	2.75	0	0
P9	Male	c.466C>A	5.33	6.67	1.33	8	4
				7.08	1.75	8	4
P10	Male	c.622C>T	4.25	6.58	2.33	7	3
				7.42	3.17	6	2
P11	Male	c.622C>T / c.509–1G>C	4.58	5.08	0.50	3	1
				5.50	0.92	2	1
				6.00	1.42	1	1
				6.42	1.83	1	1
P12	Male	c.622C>T	4.58	7.50	2.92	2	1
				8.75	4.17	2	1
				9.67	5.08	2	1
P13	Female	c.622C>T	5.42	9.50	4.08	0	0
				10.92	5.50	1	1
P14	Female	c.622C>T / c. 1523A>G	6.33	8.25	1.92	3	1

(*Continued*)

Table 1 (Continued).

ID	Gender	Genotype	Age at First Brineura Treatment (years)	Age at Examination (years)	Duration of Treatment (Years)	Weill Cornell LINCL Scale Score	HML Scale Score
P15	Female	c.509-1G>C	5.17	9.25	4.08	5	3
				11.08	5.92	4	3
P16	Male	c.622C>T	0.58	2.00	1.42	12	6
				2.42	1.83	12	6
				3.42	2.83	12	6
P17	male	c.622C>T	3.25	3.67	0.42	12	6
				4.58	1.33	10	5
				5.58	2.33	10	5
P18	Female	c.622C>T	4.17	8.33	4.17	6	2
P19	Male	c.466C>A	2.42	3.33	0.92	12	6
				3.83	1.42	12	6
				4.33	1.92	12	6
P20	Male	c.622C>T / c.509–1G>C	4.17	5.08	0.92	7	3

Abbreviations: Weill Cornell LINCL Scale score, Weill Cornell Late Infantile Neuronal Ceroid Lipofuscinosis Scale score; HML Scale score, Hamburg Motor and Language Scale score.

Study Procedures

Patients underwent OCT imaging during general anesthesia using a Spectral Domain OCT (Heidelberg Engineering OCT2 Flex, Heidelberg Engineering Inc., Heidelberg, Germany). PRNFL layer segmentation values and CRT calculation were manually confirmed with the help of the provided software (Heidelberg Eye Explorer 1.10.12.0). CRT, global (average) pRNFL (G-pRNFL), and the pRNFL values in each of the six sectors around the optic nerve head [temporal superior pRNFL (TS-pRNFL), temporal pRNFL (T-pRNFL), temporal inferior pRNFL (TI-pRNFL), nasal superior pRNFL (NS-pRNFL), nasal pRNFL (N-pRNFL) and nasal inferior pRNFL (NI-pRNFL)] were similar for both eyes of each patient and considering the disease's symmetrical progression of retinal degeneration,[7] they were averaged. Normative CRT and pRNFL thickness values in healthy children were obtained from data presented by Turk et al.[24] They assessed normative CRT and pRNFL values in a cohort of 107 healthy children using a Spectral Domain OCT device manufactured by the same manufacturer as the OCT2 Flex module utilized in our study (Heidelberg Engineering, Heidelberg, Germany). Medical history data were obtained from the DEM-CHILD database (ClinicalTrials.gov identifier NCT04613089). Each patient's neurological disease progression was quantitatively assessed by a pediatric neurologist from the NCL-specialty clinic utilizing the disease specific Weill Cornell LINCL Scale, and HML Scale.[5,25]

Statistical Analysis

Statistical analyses were performed using SPSS ver. 27.0 (IBM, Armonk, NY, USA). A two-sided *t*-test was applied to analyze differences between the observed cohort and the control group. Each statistical variable was tested for normality with a Shapiro–Wilk test. In accordance with the results, non-parametric correlation analysis (two-sided Spearman rank correlation) was performed.

Results

Participants

A total of 40 eyes of 20 patients were examined at least once and were included in this observational study. Our cohort included 12 (60%) male patients and 8 (40%) female patients. Mean age at examination was 6.90 years (range 2–11.08 years, SD 2.36) for all patients. All patients started receiving cerliponase alfa treatment prior to the presented examinations at a mean age of 4.40 years (range 0.58–6.75 years, SD 1.36).

Fourteen patients underwent serial examinations, whereas 6 patients were only examined once, resulting in a total of 84 OCT scans, 42 Weill Cornell LINCL Scale, and 42 hML Scale scores. Follow-up examinations were performed at a mean time of 1.38 years (range 0.42–2.17 years, SD 0.50). The patient's data sets are displayed in detail in Tables 1 and 2.

Table 2 Patients' Age, CRT and RNFL Values

ID	Age at Examination (Years)	Global RNFL	Temporal RNFL	Temporal Superior RNFL	Temporal Inferior RNFL	Nasal RNFL	Nasal Superior RNFL	Nasal Inferior RNFL	CRT
P1	6.83	82	72	91	89	67	85	112	100
	7.33	82	68	104	109	58	96	95	93
	8.25	77	65	92	98	51	102	88	96
P2	4.42	84	68	111	74	61	93	137	211
P3	7.75	83	76	104	103	71	86	81	125
P4	8.33	86	61	128	120	66	85	104	270
	9.33	85	63	99	115	71	116	81	270
P5	8.17	76	81	114	95	45	88	62	105
P6	9.25	62	57	85	73	55	63	46	88
	10.17	63	69	77	74	54	62	48	94
	11.00	71	68	83	87	64	65	66	99
P7	5.17	83	68	104	116	69	89	85	108
	7.00	77	67	112	115	51	72	85	110
P8	6.75	61	60	64	66	54	69	57	173
	7.67	61	63	68	74	48	64	57	157
P9	6.67	83	80	110	113	50	98	81	247
	7.08	82	78	101	93	59	86	103	242
P10	6.58	80	74	102	122	57	71	82	182
	7.42	72	66	86	122	47	58	81	136
P11	5.08	66	73	80	85	49	59	60	192
	5.50	67	66	71	89	53	71	64	181
	6.00	61	62	68	84	46	63	55	159
	6.42	60	60	80	74	44	69	53	154

(*Continued*)

Table 2 (Continued).

ID	Age at Examination (Years)	Global RNFL	Temporal RNFL	Temporal Superior RNFL	Temporal Inferior RNFL	Nasal RNFL	Nasal Superior RNFL	Nasal Inferior RNFL	CRT
P12	7.50	43	46	42	55	34	39	50	117
	8.75	55	54	57	64	48	54	61	101
	9.67	53	46	60	58	50	50	64	96
P13	9.50	74	79	72	83	67	69	77	115
	10.92	63	65	64	83	50	58	70	171
P14	8.25	79	80	72	80	65	65	129	213
P15	9.25	87	100	89	111	64	85	81	126
	11.08	79	88	91	97	54	83	74	142
P16	2.00	93	64	129	132	68	112	112	233
	2.42	90	72	129	135	60	101	93	229
	3.42	103	89	121	117	85	108	129	205
P17	3.67	99	98	122	129	63	73	146	242
	4.58	84	87	104	108	49	69	119	212
	5.58	85	74	96	98	62	74	139	195
P18	8.33	70	54	111	92	51	85	62	124
P19	3.33	92	83	106	115	73	113	90	246
	3.83	97	66	119	157	74	100	122	245
	4.33	98	73	118	112	79	107	138	252
P20	5.08	87	87	117	157	48	71	83	164

Note: RNFL and CRT values in μm.
Abbreviations: RNFL, Retinal nerve fiber layer; CRT, Central retinal thickness.

Global RNFL Assessment

Mean G-pRNFL thickness was 77.02 μm (range: 43–103, SD 13.61), displaying a significant decrease ($p < 0.0001$) compared to the normative values described by Turk et al[24] (Table 3). Thirty-nine out of the 42 measured G-pRNFL thickness values (92.86%) were beneath the normative range. The youngest patient with measurable G-pRNFL loss was 2 years of age. G-pRNFL thickness values demonstrated a very strong positive correlation with the disease-specific clinical rating scales,[26] exhibiting a Spearman correlation coefficient (r_s) of 0.849 ($p < 0.01$) for the Weill Cornell LINCL Scale, and 0.833 ($p < 0.01$) for the HML Scale. When correlated with age at examination, G-pRNFL displayed a significant negative correlation ($r_s = -0.557$, $p < 0.01$).

Evaluation of RNFL Sectors

A detailed evaluation of pRNFL sectors was performed in order to identify the different structural changes in each sector. The descriptive statistics for these values, and for the normative values for each sector[24] are illustrated in Table 3. Because clinically relevant pRNFL alterations are primarily observed in the temporal sectors of the optic nerve head, further assessment and correlation analysis will be focused on these sectors.

Table 3 Descriptive Statistics of RNFL Thickness and CRT Values in Children with Late Infantile CLN2 Disease and in Healthy Children

	CLN2 Patients	Normative Data (Turk et al, 2012)[24]	P Value
	Total (n = 42)	Total (n = 107)	
Global RNFL	77.02 ± 13.61 (43–103)	106.45 ± 9.41 (83.33–141.17)	< 0.0001**
Temporal RNFL	70.71 ± 12.19 (46–100)	74.31 ± 9.45 (53–106)	0.0566
Temporal Superior RNFL	94.12 ± 22.07 (42–129)	138.97 ± 17.58 (104–191)	< 0.0001**
Temporal Inferior RNFL	99.36 ± 24.42 (55–157)	144.64 ± 17.16 (110–183)	< 0.0001**
Nasal RNFL	57.95 ± 10.71 (34–85)	71.54 ± 10.03 (49–102)	< 0.0001**
Nasal Superior RNFL	79.19 ± 18.77 (39–116)	102.84 ± 15.96 (78–145)	< 0.0001**
Nasal Inferior RNFL	86.24 ± 28.13 (46–146)	106.4 ± 19.13 (78–162)	< 0.0001**
Central retinal thickness	167.14 ± 58.35 (88–270)	258.6 ± 17.2 (214–301)	< 0.0001**

Notes: RNFL and CRT values in μm, mean ± SD (range); **: Correlation is significant at the 0.01 level (2 – tailed).
Abbreviations: RNFL, Retinal nerve fiber layer; CRT, Central retinal thickness.

Mean TS-pRNFL and TI-pRNFL thickness values were 94.12 μm (range: 42–129, SD: 22.07) and 99.36 μm (range: 55–157, SD: 24.42) respectively, exhibiting a significant reduction ($p < 0.0001$) from the normative values,[24] with 38 TS-pRNFL values (90.48%) and 37 TI-pRNFL values (88.10%) falling below the normative range. Both TS-pRNFL and TI-pRNFL displayed moderate, significant positive correlations towards the clinical scores. Spearman correlation coefficient of TS-pRNFL was 0.788 ($p < 0.01$) for the Weill Cornell LINCL Scale and 0.739 ($p < 0.01$) for the HML Scale, whereas TI-pRNFL presented r_s values of 0.709 ($p < 0.01$) for the Weill Cornell LINCL Scale and 0.653 ($p < 0.01$) for the HML Scale. In the temporal sector, T-pRNFL thickness revealed a mean of 70.71 μm (range: 46–100, SD: 12.19). T-pRNFL values did not show any significant difference ($p < 0.0566$) when compared to healthy children,[24] as 12 of the 42 T-pRNFL values (28.57%) were below the normal range. Furthermore, T-pRNFL displayed fair, positive correlations towards the Weil Cornell LINCL Scale ($r_s = 0.389$, $p < 0.05$) and the HML Scale ($r_s = 0.417$, $p < 0.01$).

In addition to these assessments, we analyzed the correlation between pRNFL thickness values in the above sectors and the age at examination. Our data indicated that TS-pRNFL ($r_s = -0.553$, $p < 0.01$) and TI-pRNFL ($r_s = -0.504$, $p < 0.01$) exhibited significant, negative correlations towards the age at examination. T-pRNFL did not show any significant correlation to age ($r_s = -0.259$, $p > 0.05$). The correlation coefficient values for all pRNFL sectors in regard to age at examination, the Weill Cornell LINCL Scale and the HML Scale are showcased in Table 4.

Central Retinal Thickness Analysis

Our patient cohort reported a mean CRT of 167.14 (range: 88–270, SD: 58.35), demonstrating a significant decrease ($p < 0.0001$) compared to healthy children, as 34 of the 42 CRT measurements (80.95%) were lower than the normative range[24] (Table 3). The earliest age at which CRT loss was documented in our cohort was 2 years. When studying the correlation between CRT and the disease-specific clinical Scales, we discovered that CRT correlated fairly with the Weill Cornell LINCL Scale ($r_s = 0.578$, $p < 0.01$) and the HML Scale ($r_s = 0.577$, $p < 0.01$) while also demonstrating a fair negative correlation with age at examination ($r_s = -0.549$, $p < 0.01$) (Table 4).

Discussion

Late-infantile neuronal ceroid lipofuscinosis type 2 (CLN2) is a progressive neurodegenerative disorder manifesting with seizures, motor deficits, language impairment and vision loss.[4] Outer retinal degeneration has been a well-documented feature of this disease.[6–8] However, few studies have suggested inner retinal involvement.[3] In the herein study, we

Table 4 Spearman Correlation Coefficient (R_s) Values Between RNFL Thickness and CRT Values, Age at Examination, Weill Cornell LINCL Scale Scores, and HML Scale Scores

	Age at Examination (Years)	Weill Cornell LINCL Scale Score	HML Scale Score
Global RNFL	−0.557**	0.849**	0.833**
Temporal RNFL	−0.259	0.389*	0.417**
Temporal Superior RNFL	−0.553**	0.788**	0.739**
Temporal Inferior RNFL	−0.504**	0.709**	0.653**
Nasal RNFL	−0.209	0.541**	0.500**
Nasal Superior RNFL	−0.437**	0.654**	0.674**
Nasal Inferior RNFL	−0.522**	0.738**	0.707**
Central retinal thickness	−0.549**	0.578**	0.577**

Notes: *: Correlation is significant at the 0.05 level (2-tailed); **: Correlation is significant at the 0.01 level (2 – tailed).
Abbreviations: RNFL, Retinal nerve fiber layer; CRT, Central retinal thickness; Weill Cornell LINCL Scale score, Weill Cornell Late Infantile Neuronal Ceroid Lipofuscinosis Scale score; HML Scale score, Hamburg Motor and Language Scale score.

identified the presence of progressive pRNFL degeneration in treatment experienced patients with genetically confirmed diagnosis of late-infantile CLN2 disease.

Natural history studies on the disease's ocular manifestations have described a bilateral and symmetrical,[7] progressive retinal degeneration that commences from the macula and expands to the peripheral retina in a bull's eye pattern.[6] This degenerative process, which is especially amplified during the pivotal period of 48 to 72 months[7] is initially identifiable in the parafoveal area, at the layer of the photoreceptors, the RPE,[6] and the ONL layer, which precedes EZ loss.[3] These parafoveal changes progress further to the fovea, and subsequently to the outer macula,[3] before ultimately advancing centrifugally to the peripheral retina.

Currently, ICV ERT with cerliponase alfa is the only US FDA and EMA approved treatment that slows the progression of neurological decline in late-infantile CLN2 disease.[9] However, studies on treatment experienced patients have illustrated the ineffectiveness of ICV infusions in mitigating retinal impairment in the context of this disease. In a previous investigation, our team highlighted that despite undergoing ICV ERT treatment, patients still exhibited a continuous decline in CRT, with a marked increase in the deterioration rate between 56 and 80 months of age.[8] Recently, Huang et al reaffirmed through OCT analyses that treatment experienced patients display the same pattern of outer retinal deterioration, which is observed in natural history studies.[3,14] Introducing a novel OCT-based clinical staging system, the authors illustrated parafoveal changes and foveal sparing in stage 2, followed by foveal involvement in stage 3, and eventually global macular degeneration, in stages 4 and 5.[14] In the herein study, we were able to further reinforce these findings by revealing a significant decrease in the CRT values of our treatment experienced cohort. Moreover, we found a significant inverse association between CRT and the age at examination, confirming the results of Kovacs et al,[7] and of our previous investigation.[8]

Although the investigation of inner retinal alterations in late-infantile CLN2 disease has comparably received less attention, electroretinography (ERG) studies on treatment naïve LINCL patients[27] and CLN2 canine models[28] provided results supporting inner retinal involvement in this neurodegenerative disease. Additionally, Katz et al[29] identified inner nuclear layer (INL) degeneration and accumulation of fluorescent lysosomal storage material in canine retinal ganglion cells, and in a later OCT natural history study, Kovacs et al suggested that RNFL may be affected in advanced stages of the disease as well.[3] Nevertheless, conflicting evidence from preclinical[28] and clinical studies alike[7,14] have led to a lack of consensus within the scientific community regarding RNFL loss in late-infantile CLN2 disease.

In our present analysis of 84 OCT scans of 20 late-infantile CLN2 patients we identified that pRNFL thickness values were significantly decreased when compared to healthy children. Furthermore, we discovered that despite treatment,

retinal ganglion cell axons followed a significant inverse association in correlation to age (Figure 1). The presence of pRNFL thinning was observable in patients as young as 2 years of age, before the onset of the rapid retinal decline period and preceding the presentation of motor and language deficits. These findings challenge the conclusions drawn by Kovacs et, who described the absence of pRNFL thinning during the early stages of outer retinal degeneration, suggesting that pRNFL loss manifests in advanced stages of the disease, after the age of 5 years.[3] Our outcomes of progressive pRNFL degeneration in late-infantile CLN2 are consistent with the documented nerve fiber layer loss, exhibited in other neurodegenerative metabolic diseases. Characteristically, pRNFL thinning has been recognized in patients with type 1 Gaucher disease (GD1), Adrenoleukodystrophy (ALD) and Wilson's Disease (WD) alike.[30–32]

Subsequently, we explored the potential relationship between pRNFL degeneration and clinical deterioration in regard to patient's motor and language functions, as assessed via the disease specific Weill Cornell LINCL and HML clinical rating Scales. Our analysis concluded that the severity of pRNFL degeneration correlates very strongly with the decline in neurological function, as patients with the lowest pRNFL thickness values displayed the worst clinical symptoms. Even though CRT values also correlated significantly with the clinical scores, their correlation coefficients were inferior to those established by pRNFL (Table 4).

Notably, it became evident during our study that the temporal sector was the only sub – sector that did not display a significant nerve fiber loss compared to healthy controls. Furthermore, T-pRNFL thickness values did not demonstrate a significant correlation towards the age at examination, in contrast to the strong negative linear relationship displayed between TS-pRNFL and TI-pRNFL and age (Figure 2). These differences became even more profound when we examined the relationship between pRNFL loss in each sector and the patient's neurological status, as pRNFL thickness

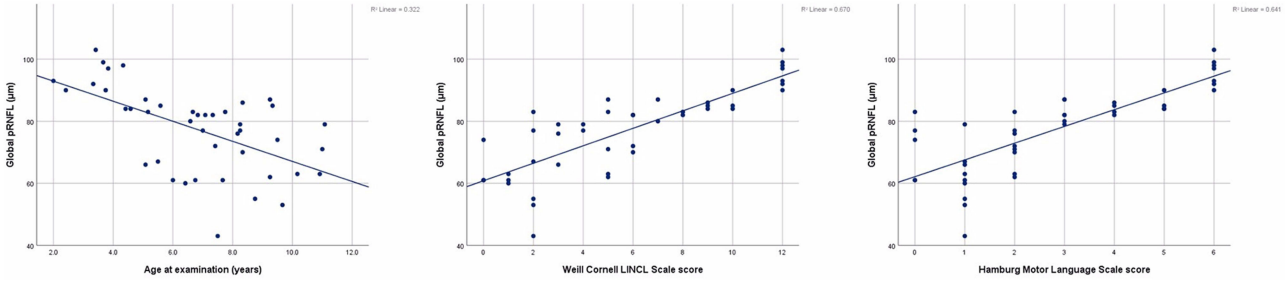

Figure 1 Global RNFL values correlated with age at examination, the Weill Cornell Clinical Scale scores and the Hamburg Motor Language Scale scores.

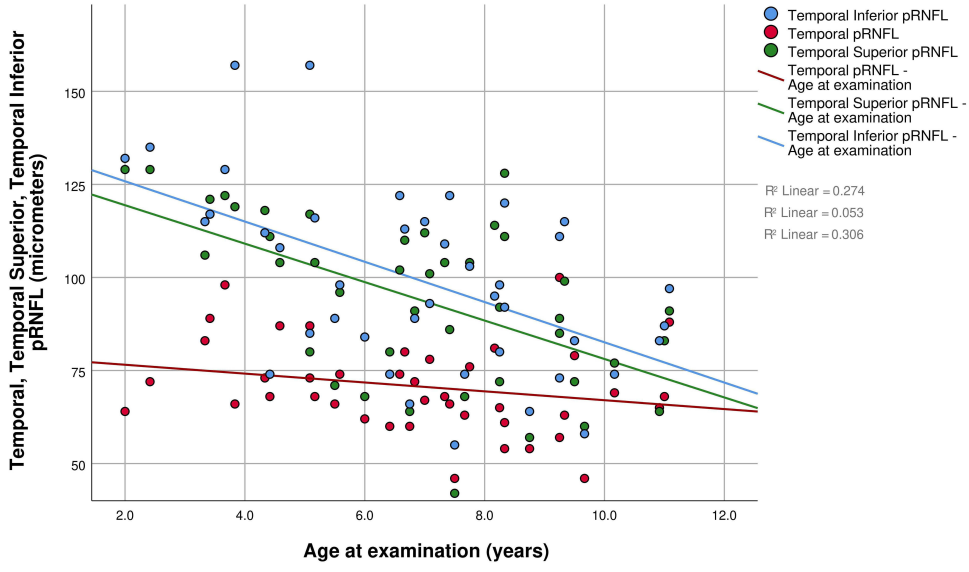

Figure 2 Temporal, Temporal Superior and Temporal Inferior pRNFL values correlated with age at examination.

values in the temporal superior and temporal inferior sectors exhibited greater correlations towards the Weil Cornell LINCL and HML Scales, compared to those in the temporal sector. These findings suggest that in late-infantile CLN2 disease pRNFL loss occurs predominantly in the superotemporal and inferotemporal region, whereas the temporal nerve fibers are relatively preserved throughout the disease (Figure 3). This regional pattern of retinal nerve fiber loss is similar to the sectoral neurodegeneration trend described in glaucoma, where pRNFL thinning is primarily observed in the temporal superior and temporal inferior sectors and the temporal sector is generally spared until the later stages of disease.[33,34] The notion behind this specific pattern of sectoral degeneration, which has been identified in other neurodegenerative diseases as well, including Alzheimer's disease,[35] is still unclear.[36] It has been suggested that neurodegeneration in the superior and inferior quadrants may be more profound, because of the larger number of neurons that are naturally located in these regions, compared to the temporal retina.[37] Furthermore, the difference between the size and the axons length of the bigger parasol cells (M – cells) that are primarily located superiorly and inferiorly, and the smaller midget cells (P – cells) which are mainly found in the temporal sector may affect cellular susceptibility to amyloid deposition, metabolic requirements, and myelin sheath turnover.[35,36] These considerations, together with other potential factors including differences in vascularization and glial cell support could impact the degenerative process, culminating in the distinctive pattern of neurodegeneration described above.[35]

Based on our findings, we support the notion that progressive pRNFL loss in late-infantile CLN2 disease is primarily the result of CNS driven neurodegeneration and not secondary to outer retinal degeneration. The detection of pathologic pRNFL thickness values in patients as young as 2 years of age, combined with the presence of pRNFL deterioration in patients with preserved CRT values suggest that RNFL degeneration may occur concurrently with, or even prior to perifoveal outer retinal alterations.

In addition, an analysis of the pRNFL sectors highlighted that the temporal superior and temporal inferior sectors were the first, as well as the most frequently affected regions by the RNFL degeneration, in contrast to the temporal nerve fibers which comparably appeared unimpaired. These observations challenge the assumption that pRNFL loss in late-infantile CLN2 disease occurs as a secondary effect to macular degeneration, as if that would be the case, then

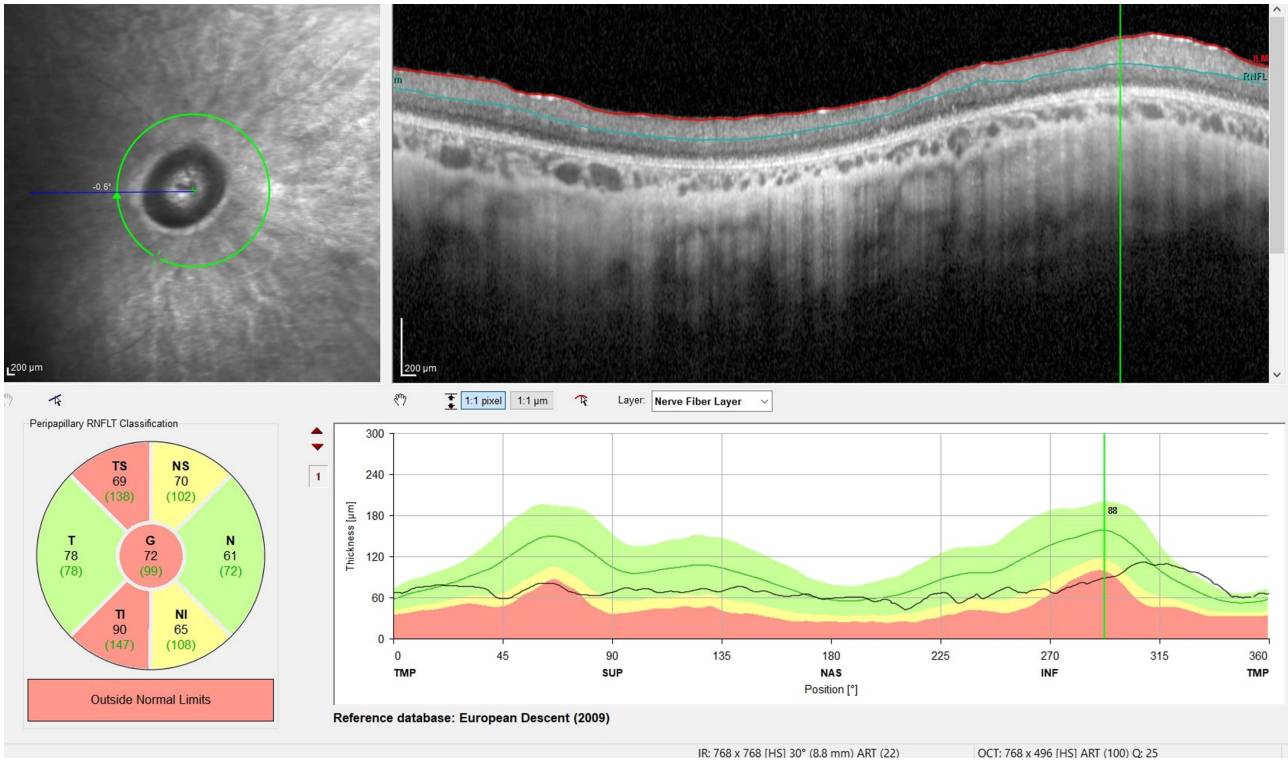

Figure 3 Heidelberg SD-OCT RNFL analysis of a 9.5-year-old patient with late-infantile CLN2 disease. PRNFL is significantly decreased in the global, temporal superior and temporal inferior pRNFL sectors.

neurodegeneration would primarily affect the papillomacular bundle and manifest as temporal pRNFL loss.[35,38] Retinal ganglion cell pathology appears to occur independently of outer retina pathology.

The strong interrelation between CNS and pRNFL deterioration, in combination with our findings may suggest that pRNFL loss could be a direct result of the neurodegeneration in late-infantile CLN2 disease and not a secondary feature to retinal degeneration. The potential of OCT assessed pRNFL thickness could add value as a potential biomarker for monitoring and predicting neurodegenerative progression and evaluating response to treatment. The effectiveness of RNFL as a surrogate for disease progression has been extensively studied in several metabolic, and non-metabolic neurodegenerative diseases including Niemann – Pick type C disease, Wilson's Disease, Huntington Disease and more.[15,22,39–41] The substantial body of research on the potential of RNFL as a biomarker is plausible considering its fast and noninvasive nature, its repeatability, and its reproducibility.[42,43]

Based on the outcomes of the herein study, we believe that OCT analysis of pRNFL thickness is a reliable, noninvasive tool that can contribute significantly to the tracking of disease progression in treatment experienced, and inexperienced patients, as well as in the development of new disease modifying treatment approaches.

The herein investigation represents one of the largest studies on the ocular manifestations of late-infantile CLN2 disease, considering the rarity of the disease and the low compliance rate of patients, on account of the occurring CNS degeneration. However, a larger sample size and additional prospective longitudinal examinations would still be required in order to reinforce the findings of our study. In light of these limitations, we strongly encourage further investigations on RNFL alterations in late-infantile CLN2 patients, as well as further studies on the correlation of RNFL changes and CNS degeneration in the framework of this disease. In view of the detected degeneration of various retinal layers in CLN2 disease, ophthalmic examination including OCT imaging should be part of follow-up visits in CLN2 patients.

Data Sharing Statement

No additional data will be made available.

Disclosure

Dr Miriam Nickel reports personal fees from RegenxBio, during the conduct of the study; grants, personal fees from BioMarin, outside the submitted work. Dr Angela Schulz reports personal fees from RegenxBio, during the conduct of the study; grants, personal fees from BioMarin, outside the submitted work. The authors declare no other financial interests or conflicts of interest related to the presented data.

References

1. Bartsch U, Storch S. Experimental therapeutic approaches for the treatment of retinal pathology in neuronal ceroid lipofuscinoses. *Front Neurol*. 2022;13:866983. doi:10.3389/fneur.2022.866983
2. Kaminiów K, Kozak S, Paprocka J. Recent insight into the genetic basis, clinical features, and diagnostic methods for neuronal ceroid lipofuscinosis. *Int J Mol Sci*. 2022;23(10):5729. doi:10.3390/ijms23105729
3. Kovacs KD, Orlin A, Sondhi D, et al. Automated retinal layer segmentation in *CLN2* -associated disease: commercially available software characterizing a progressive maculopathy. *Trans Vision Sci Technol*. 2021;10(8):23. doi:10.1167/tvst.10.8.23
4. Nickel M, Simonati A, Jacoby D, et al. Disease characteristics and progression in patients with late-infantile neuronal ceroid lipofuscinosis type 2 (CLN2) disease: an observational cohort study. *Lancet Child Adolesc Health*. 2018;2(8):582–590. doi:10.1016/S2352-4642(18)30179-2
5. Worgall S, Kekatpure MV, Heier L, et al. Neurological deterioration in late infantile neuronal ceroid lipofuscinosis. *Neurology*. 2007;69 (6):521–535. doi:10.1212/01.wnl.0000267885.47092.40
6. Orlin A, Sondhi D, Witmer MT, et al. Spectrum of ocular manifestations in CLN2-associated batten (Jansky-Bielschowsky) disease correlate with advancing age and deteriorating neurological function. *PLoS One*. 2013;8(8):e73128. doi:10.1371/journal.pone.0073128
7. Kovacs KD, Patel S, Orlin A, et al. Symmetric age association of retinal degeneration in patients with CLN2-associated batten disease. *Ophthalmol Retina*. 2020;4(7):728–736. doi:10.1016/j.oret.2020.01.011
8. Dulz S, Schwering C, Wildner J, et al. Ongoing retinal degeneration despite intraventricular enzyme replacement therapy with cerliponase alfa in late-infantile neuronal ceroid lipofuscinosis type 2 (CLN2 disease). *Br J Ophthalmol*. 2023;107(10):1478–1483. doi:10.1136/bjo-2022-321260
9. Schulz A, Ajayi T, Specchio N, et al. Study of intraventricular cerliponase alfa for CLN2 disease. *N Engl J Med*. 2018;378(20):1898–1907. doi:10.1056/NEJMoa1712649
10. Tracy CJ, Whiting REH, Pearce JW, et al. Intravitreal implantation of TPP1-transduced stem cells delays retinal degeneration in canine CLN2 neuronal ceroid lipofuscinosis. *Exp Eye Res*. 2016;152:77–87. doi:10.1016/j.exer.2016.09.003
11. Kick GR, Whiting REH, Ota-Kuroki J, et al. Intravitreal gene therapy preserves retinal function in a canine model of CLN2 neuronal ceroid lipofuscinosis. *Exp Eye Res*. 2023;226:109344. doi:10.1016/j.exer.2022.109344

12. Whiting REH, Robinson Kick G, Ota-Kuroki J, et al. Intravitreal enzyme replacement inhibits progression of retinal degeneration in canine CLN2 neuronal ceroid lipofuscinosis. *Exp Eye Res*. 2020;198:108135. doi:10.1016/j.exer.2020.108135
13. Henderson R, Wawrzynski J, Rodriguez Martinez A, et al. Intravitreal cerliponase alfa slows the rate of retinal thinning in patients with CLN2 type batten disease: a first in man report. *Invest Ophthalmol Visual Sci*. 2023;64(8):788.
14. Huang WC, Atiskova Y, Ohnsman CM, Dulz S. OCT biomarkers in ocular CLN2 disease. *Invest Ophthalmol Visual Sci*. 2021;62(8):2448.
15. Al-Mujaini AS, Al-Mujaini MS, Sabt BI. Retinal nerve fiber layer thickness in multiple sclerosis with and without optic neuritis: a four-year follow-up study from Oman. *BMC Ophthalmol*. 2021;21(1):391. doi:10.1186/s12886-021-02158-0
16. Cilingir V, Batur M. First measured retinal nerve fiber layer thickness in RRMS can be used as a biomarker for the course of the disease: threshold value discussions. *J Neurol*. 2021;268(8):2858–2865. doi:10.1007/s00415-021-10469-x
17. El-Kattan MM, Esmat SM, Esmail EH, Deraz HA, Ismail RS. Optical coherence tomography in patients with Parkinson's disease. *Egyptian J Neurol Psychiatry Neurosurg*. 2022;58(1):21. doi:10.1186/s41983-021-00421-1
18. J-g Y, Y-f F, Xiang Y, et al. Retinal nerve fiber layer thickness changes in Parkinson disease: a meta-analysis. *PLoS One*. 2014;9(1):e85718. doi:10.1371/journal.pone.0085718
19. T-h L, Jin Z, Y-z Q, et al. The relationship between retinal nerve fiber layer thickness and clinical symptoms of Alzheimer's disease. *Front Aging Neurosci*. 2021;12:584244. doi:10.3389/fnagi.2020.584244
20. Moreno-Ramos T, Benito-León J, Villarejo A, Bermejo-Pareja F. Retinal nerve fiber layer thinning in dementia associated with Parkinson's disease, dementia with Lewy bodies, and Alzheimer's disease. *J Alzheimers Dis*. 2013;34(3):659–664. doi:10.3233/JAD-121975
21. Glasner P, Sabisz A, Chylińska M, Komendziński J, Wyszomirski A, Karaszewski B. Retinal nerve fiber and ganglion cell complex layer thicknesses mirror brain atrophy in patients with relapsing-remitting multiple sclerosis. *Restorat Neurol Neurosci*. 2022;40(1):35–42. doi:10.3233/RNN-211176
22. Jiménez B, Ascaso FJ, Cristóbal JA, López Del Val J. Development of a prediction formula of Parkinson disease severity by optical coherence tomography. *Mov Disord*. 2014;29(1):68–74. doi:10.1002/mds.25747
23. Wyrwich KW, Schulz A, Nickel M, et al. An adapted clinical measurement tool for the key symptoms of CLN2 disease. *J Inborn Error Metabol Screen*. 2018;6:232640981878838. doi:10.1177/2326409818788382
24. Turk A, Ceylan OM, Arici C, et al. Evaluation of the nerve fiber layer and macula in the eyes of healthy children using spectral-domain optical coherence tomography. *Am J Ophthalmol*. 2012;153(3):552–559e551. doi:10.1016/j.ajo.2011.08.026
25. Wyrwich KW, Schulz A, Nickel M, et al. An adapted clinical measurement tool for the key symptoms of CLN2 disease. *Sage J*. 2018;6:2326409818788382.
26. Akoglu H. User's guide to correlation coefficients. *Turkish J Emerg Med*. 2018;18(3):91–93. doi:10.1016/j.tjem.2018.08.001
27. Weleber RG. The dystrophic retina in multisystem disorders: the electroretinogram in neuronal ceroid lipofuscinoses. *Eye*. 1998;12(3):580–590. doi:10.1038/eye.1998.148
28. Whiting REH, Narfström K, Yao G, et al. Enzyme replacement therapy delays pupillary light reflex deficits in a canine model of late infantile neuronal ceroid lipofuscinosis. *Exp Eye Res*. 2014;125:164–172. doi:10.1016/j.exer.2014.06.008
29. Katz ML, Coates JR, Cooper JJ, O'Brien DP, Jeong M, Narfstro¨m K. Retinal pathology in a canine model of late infantile neuronal ceroid lipofuscinosis. *Investigat Opthalmol Vis Sci*. 2008;49(6):2686. doi:10.1167/iovs.08-1712
30. Weill Y, Zimran A, Zadok D, et al. Macular ganglion cell complex and peripapillary retinal nerve fiber layer thinning in patients with type-1 Gaucher disease. *Int J Mol Sci*. 2020;21(19):7027. doi:10.3390/ijms21197027
31. Albrecht P, Müller A-K, Ringelstein M, et al. Retinal neurodegeneration in Wilson's Disease revealed by spectral domain optical coherence tomography. *PLoS One*. 2012;7(11):e49825. doi:10.1371/journal.pone.0049825
32. Van Ballegoij WJC, Huffnagel IC, Van De Stadt SIW, et al. Optical coherence tomography to measure the progression of myelopathy in adrenoleukodystrophy. *Ann Clin Transl Neurol*. 2021;8(5):1064–1072. doi:10.1002/acn3.51349
33. Lee VW, Mok KH. Retinal nerve fiber layer measurement by nerve fiber analyzer in normal subjects and patients with glaucoma. *Ophthalmology*. 1999;106(5):1006–1008. doi:10.1016/S0161-6420(99)00524-2
34. Baniasadi N, Paschalis EI, Haghzadeh M, et al. Patterns of retinal nerve fiber layer loss in different subtypes of open angle glaucoma using spectral domain optical coherence tomography. *J Glaucoma*. 2016;25(10):865–872. doi:10.1097/IJG.0000000000000534
35. La Morgia C, Di Vito L, Carelli V, Carbonelli M. Patterns of retinal ganglion cell damage in neurodegenerative disorders: parvocellular vs magnocellular degeneration in optical coherence tomography studies. *Front Neurol*. 2017;8:710. doi:10.3389/fneur.2017.00710
36. Kim US, Mahroo OA, Mollon JD, Yu-Wai-Man P. Retinal ganglion cells—diversity of cell types and clinical relevance. *Front Neurol*. 2021;12:661938. doi:10.3389/fneur.2021.661938
37. Den Haan J, Verbraak FD, Visser PJ, Bouwman FH. Retinal thickness in Alzheimer's disease: a systematic review and meta-analysis. *Alzheimers Dement*. 2017;6(1):162–170.
38. Leung CKS, Guo PY, Lam AKN. Retinal nerve fiber layer optical texture analysis. *Ophthalmology*. 2022;129(9):1043–1055. doi:10.1016/j.ophtha.2022.04.012
39. Havla J, Moser M, Sztatecsny C, et al. Retinal axonal degeneration in Niemann–Pick type C disease. *J Neurol*. 2020;267(7):2070–2082. doi:10.1007/s00415-020-09796-2
40. Mutlu U, Colijn JM, Ikram MA, et al. Association of retinal neurodegeneration on optical coherence tomography with dementia: a population-based study. *JAMA neurol*. 2018;75(10):1256. doi:10.1001/jamaneurol.2018.1563
41. Langwińska-Wośko E, Litwin T, Dzieżyc K, Karlinski M, Członkowska A. Optical coherence tomography as a marker of neurodegeneration in patients with Wilson's disease. *Acta Neurologica Belgica*. 2017;117(4):867–871. doi:10.1007/s13760-017-0788-5
42. Maldonado RS, Mettu P, El-Dairi M, Bhatti MT. The application of optical coherence tomography in neurologic diseases. *Neurol Clin Pract*. 2015;5(5):460–469. doi:10.1212/CPJ.0000000000000187
43. Loh EH-T, Ong Y-T, Venketasubramanian N, et al. Repeatability and reproducibility of retinal neuronal and axonal measures on spectral-domain optical coherence tomography in patients with cognitive impairment. *Front Neurol*. 2017;8:359. doi:10.3389/fneur.2017.00359